Development 133, 3399-3409 (2006) doi:10.1242/dev.02497

Smad5 determines murine amnion fate through the control of bone morphogenetic protein expression and signalling levels

Erika A. Bosman[1,*], Kirstie A. Lawson[2,†], Joke Debruyn[1], Lisette Beek[1], Annick Francis[1], Luc Schoonjans[3], Danny Huylebroeck[1] and An Zwijsen[1,‡]

Smad5 is an intracellular mediator of bone morphogenetic protein (Bmp) signalling. It is essential for primordial germ cell (PGC) development, for the development of the allantois and for amnion closure, as demonstrated by loss of Bmp signalling. By contrast, the appearance of ectopic PGC-like cells and regionalized ectopic vasculogenesis and haematopoiesis in thickened *Smad5*$^{m1/m1}$ amnion are amnion defects that have not been associated with loss of Bmp signalling components. We show that defects in amnion and allantois can already be detected at embryonic day (E) 7.5 in *Smad5* mutant mice. However, ectopic Oct4-positive (Oct4$^+$) and alkaline phosphatase-positive (AP$^+$) cells appear suddenly in thickened amnion at E8.5, and at a remote distance from the allantois and posterior primitive streak, suggesting a change of fate in situ. These ectopic Oct4$^+$, AP$^+$ cells appear to be *Stella* negative and hence cannot be called bona fide PGCs. We demonstrate a robust upregulation of *Bmp2* and *Bmp4* expression, as well as of Erk and Smad activity, in the *Smad5* mutant amnion. The ectopic expression of several Bmp target genes in different domains and the regionalized presence of cells of several Bmp-sensitive lineages in the mutant amnion suggest that different levels of Bmp signalling may determine cell fate. Injection of rBMP4 in the exocoelom of wild-type embryos can induce thickening of amnion, mimicking the early amnion phenotype in *Smad5* mutants. These results support a model in which loss of Smad5 results paradoxically in gain of Bmp function defects in the amnion.

KEY WORDS: Allantois, Amnion, Bmp, Chimera, PGC, Smad5/Madh5, Stem cell, Tgfβ

INTRODUCTION

In mouse embryos, extra-embryonic mesoderm cells of the prospective visceral yolk sac, chorion, allantois and amnion are among the first mesoderm cells to emerge early at gastrulation. Cell labelling studies have shown that a population of posterior and posterolateral epiblast cells that enters the primitive streak proximally will give rise to this extra-embryonic mesoderm and also to primordial germ cells (PGCs) (Lawson and Hage, 1994; Parameswaran and Tam, 1995; Kinder et al., 1999). Genetic evidence and epiblast culture experiments have shown that germ cell competence and formation of the allantois are induced in the proximal epiblast before gastrulation, in response to bone morphogenetic proteins (Bmps) produced in the extra-embryonic ectoderm, but depend also on the presence of visceral endoderm (reviewed by Zhao, 2003; de Sousa Lopes et al., 2004).

Bmps are ligands of the transforming growth factor β (Tgfβ) family that use various receptor complexes to directly activate intracellular effector proteins (Smad1/5/8). Smads transmit the signal to the nucleus and participate in the regulation of target gene expression (Shi and Massagué, 2003). Analysis of conventional knockout mice showed that the repertoire of Bmp signalling proteins involved in PGC induction comprise Bmps (Bmp2, -4 and -8b), a type I Bmp receptor (Alk2; Acvr1 – Mouse Genome Informatics) and two Bmp-Smads (Smad1/5) (Lawson et al., 1999; Ying et al., 2000; Ying et al., 2001; Ying and Zhao, 2001; Chang and Matzuk, 2001; Tremblay et al., 2001; Hayashi et al., 2002; de Sousa Lopes et al., 2004; Okamura et al., 2005). Recently, it was shown that Blimp1 (Prdm1 – Mouse Genome Informatics), a transcriptional regulator thought to be induced by Bmp4, is a key regulator of germ cell specification (Vincent et al., 2005; Ohinata et al., 2005). Subsequent PGC localization and survival, as well as allantois differentiation, also depend on the presence of Bmp4 in the extra-embryonic mesoderm (Fujiwara et al., 2001).

Several Bmps have been implicated in the specification and growth of extra-embryonic mesoderm. The induction of the allantois crucially depends on Bmp4 (Winnier et al., 1995; Fujiwara et al., 2001), and on Alk2-mediated signalling in visceral endoderm (Mishina et al., 1999; Gu et al., 1999). Bmp5;Bmp7 double mutant mouse embryos display impaired allantois maturation (Solloway and Robertson, 1999). Bmp2 plays a unique role in amnion development, as the pro-amniotic canal does not close in *Bmp2* mutant mice, which has been ascribed to reduced and thus insufficient production of extra-embryonic mesoderm (Zhang and Bradley, 1996).

Smad1 and *Smad5* null embryos die at mid-gestation and have defects in PGC specification and allocation, and in the development of extra-embryonic tissues (Chang et al., 1999; Chang et al., 2000; Yang et al., 1999; Lechleider et al., 2001; Tremblay et al., 2001; Hayashi et al., 2002; Umans et al., 2003). The presence on the amnion of aggregates of cells that contain ectopic primitive red blood cells, and endothelial and PGC-like cells, is a unique feature of *Smad5* mutants (Chang et al., 1999; Chang and Matzuk, 2001). However, the molecular mechanism underlying this unique phenotype remained unknown. Our present chimera study reveals

[1]Department of Developmental Biology (VIB7), Flanders Interuniversity Institute for Biotechnology (VIB) and Laboratory of Molecular Biology (Celgen), University of Leuven, B-3000 Leuven, Belgium. [2]Hubrecht Laboratory, Netherlands Institute of Developmental Biology, Utrecht, The Netherlands. [3]Thromb-X S.A., Leuven, Belgium.

*Present address: Wellcome Trust Sanger Institute, Hinxton, UK
†Present address: MRC Human Genetics Unit, Western General Hospital, Edinburgh, UK
‡Author for correspondence (e-mail: an.zwijsen@med.kuleuven.be)

Accepted 15 June 2006

that Smad5 functions non-cell-autonomously in the amnion mesoderm. In addition, we observe ectopic Bmp expression and signalling in the affected amnion. We therefore propose a new model in which Smad5 deficiency paradoxically leads to gain of Bmp function defects. Additional support for this model comes from injection of rBMP4 protein in the exocoelom of wild-type embryos, which results in abnormal thickening of the amnion.

MATERIALS AND METHODS

Mouse strains and production of chimeric embryos

The *Smad5^{m1}* mutation (Chang et al., 1999) was outcrossed in C57BL/6J and F2 crosses of F1 (C57BL/6J × CBA) background for at least five generations. Rosa-βgeo-26 mice, expressing *Escherichia coli lacZ* ubiquitously (Friedrich and Soriano, 1991), were maintained in the F2 background. Embryonic stem (ES) cells were established from blastocysts of *Smad5$^{+/m1}$* (C57BL/6J) intercrosses as described (Schoonjans et al., 2003), and genotyped by PCR and Southern blotting (Chang et al., 1999).

Chimeras between ES cell lines and diploid Rosa-βgeo-26 morulae were generated as described (Goumans et al., 1999). The majority of wild-type→WT^{lacZ}, *Smad5$^{+/m1}$*→WT^{lacZ}, and of *Smad5$^{m1/m1}$*→WT^{lacZ} chimeric embryos had a high ES cell contribution (>90%), with only few acceptor-morula derived, β-galactosidase-positive cells present in hindgut endoderm. The minority of *Smad5$^{m1/m1}$*→WT^{lacZ} embryos (four out of 18) with a high contribution from the wild-type acceptor morula in epiblast-derived tissues (20-80% ES cell-derived embryos) are here referred to as low-percentage chimeras.

Animal care and experiments were approved by the Institutional Ethical Committee of the Catholic University of Leuven.

Collection of post-implantation embryos, in situ hybridization and immunohistochemistry

Embryos from timed matings were dissected in ice-cold PBS at embryonic day (E) 7.0-9.5 and staged according to Downs and Davies (Downs and Davies, 1993), modified for C57BL/6 × CBA embryos (Edinburgh Mouse Atlas Project: http://genex.hgu.mrc.ac.uk/Databases/Anatomy/MAstaging.shtml), or on somite number. Radioactive in situ hybridization was performed as described (Dewulf et al., 1995). Non-radioactive in situ hybridization [*Stella* (*Dppa3* – Mouse Genome Informatics), fragilis (Ifitm3 – Mouse Genome Informatics)] on sections and immunohistochemistry for P-ERK (cat. no 9101, Cell Signalling Technologies) and P-Smad1/5/8 (cat. no 9511, Cell Signalling Technologies) were performed with the automated Ventana Discovery system and Ventana reagents according to the manufacturer's instructions. NBT/BCIP and DAB were used as chromogens for automated non-radioactive in situ hybridization and immunohistochemistry, respectively. We used antisense RNA probes for *Bmp2* (Lyons et al., 1989), *Bmp4* (Jones et al., 1991), periostin/*Osf2* (Delot et al., 2003), *Stella* and fragilis (Saitou et al., 2002), and *Msx2* (MacKenzie et al., 1992).

Immunohistochemistry for Oct4 (Pou5f1 – Mouse Genome Informatics; sc5279, Santa Cruz Biotechnology) and SSEA-1 (Fut4 – Mouse Genome Informatics; MC480 DHSB) was performed as described (Van Eynde et al., 2004). AEC (Sigma) was used as a chromogen.

Detection and counting of PGCs

Dissection of embryos, followed by fixation, and detection of alkaline phosphatase (AP)-positive PGCs with α-naphthyl phosphate/Fast Red TR (Ginsburg et al., 1990) in whole-mount embryos or with ASMX/Fast Red TR in serial section, were as described (Lawson et al., 1999). PGCs were counted on the basis of the strong surface AP staining and intensely stained cytoplasmic spot (Ginsburg et al., 1990; Lawson and Hage, 1994). The anterior portion of the embryo was retained for genotyping (Chang et al., 1999).

Measurements

Allantois dimensions were measured on intact embryos after staining for AP. The axial length of the allantois was measured from the line of intersection with the yolk sac when viewed posteriorly and from the junctional line between amnion and yolk sac when viewed laterally. Width at the base was measured in posterior view along the intersection with the yolk sac.

The length of the anterior-posterior embryonic axis was estimated on images of intact embryos stained for AP and viewed laterally. Axis length was taken as the sum of the three longest cords along the curved axis – from the anterior embryo/amnion junction or the most proximal edge of the neural fold, from the intersection of amnion, allantois and primitive streak to the node, and a cord connecting these two.

Injection of rBMP4 and whole embryo culture

CD1 embryos between neural plate (NP) and headfold (HF) stages were isolated in 22 mmol/l Hepes and 10% heat-inactivated fetal calf serum (FCS; Hyclone); Reichert's membrane was removed, but yolk sac integrity with the ectoplacental cone was maintained. Whole embryo culture and manipulations were in Dulbecco's modified essential medium (Gibco), 1 mmol/l glutamine, non-essential amino acids, 0.5 mmol/l Na-pyruvate, 50% heat-inactivated horse serum (Gibco) in a rolling culture system at 37°C and 5% CO_2 for 15 to 24 hours (0.5 ml medium per embryo). Embryos were either control injected or injected with 1 μg human rBMP4/ml PBS (R&D Systems) with a mouth-controlled glass capillary in the exocoelom (1-2 nl; corresponding to about one-tenth of the luminal volume of the exocoelom). Control injected embryos developed normally, as judged by embryo viability, somite number, axial rotation, allantois elongation and fusion, and neural tube closure. Yolk sac vasculogenesis appeared normal, but the yolk sac was sometimes enlarged when compared to freshly isolated embryos. Only embryos in which the heart was beating were assessed for amnion development. Embryos were fixed and processed for paraffin embedding.

RESULTS

Smad5$^{m1/m1}$ mouse embryos have extra-embryonic and embryonic defects

The *Smad5^{m1}* allele was bred into C57BL/6J and F2 (C57BL/6J×CBA) backgrounds to reduce phenotype variation. In both backgrounds we observed the same defects in gross morphology as in *Smad5$^{m1/m1}$* embryos in a mixed background (Chang et al., 1999), although relatively fewer mildly affected embryos were recovered and anterior defects were more pronounced (data not shown). The very first defects visible in *Smad5* mutants were the delayed appearance of the allantois at late streak (LS) stages (P<0.01 with Wilcoxon's summed ranks test) (Fig. 1A) and the relatively posterior closure of the amnion visible in late streak-early bud (LSEB) to HF stage embryos (Table 1, data not shown). The delayed appearance of the allantois was followed initially by normal extension

Table 1. Extra-embryonic defects in *Smad5$^{m1/m1}$* mutants

Extra-embryonic defects	*n*	No defects	Thickened amnion and/or abnormal allantois*	Amnion aggregates, not AP positive	Amnion aggregates, some AP positive
LS-4S	32	16 (50%)	16 (50%)	0 (0%)	0 (0%)
5-12S	8	0 (0%)	2 (25%)	1 (13%)	5 (62%)
13-28S	19	2 (11%)	2 (11%)	2 (11%)	13 (58%)

*These defects are often associated with posterior closure of the amnion (see Fig. 1D,E, Fig. 3B and Fig. 4 for examples).

DEVELOPMENT

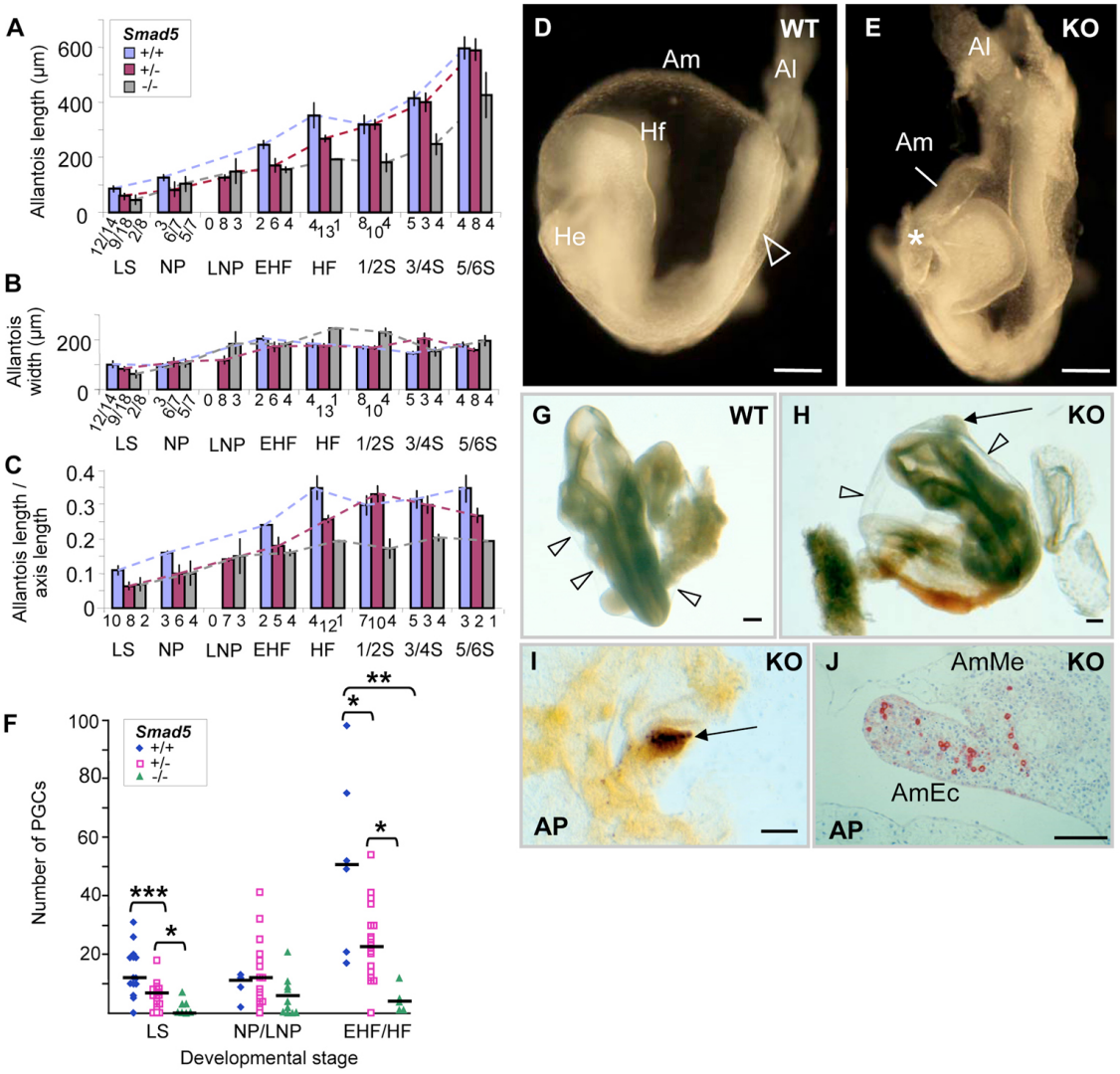

Fig. 1. Impaired allantois and PGC development in *Smad5*$^{m1/m1}$ embryos. (**A-C**) Allantois dimensions measured in embryos collected from *Smad5*$^{m1/+}$ crosses in F2 (C57BL/6J × CBA) background. Results at different developmental stages were expressed as means ± s.e. The numbers under the histogram represent the number of embryos in each group. A numerator indicates the embryos with an allantoic bud. Zero values are not included in the mean. (A) Allantois length (μm). (B) Allantois width (μm) was measured at the base of the allantois (right-left axis). (C) The ratio of the allantois length over the embryonic axis length. (**D**) Wild-type (5S) embryo with a well-developed head, hindgut entrance (open arrowhead) and heart, and an elongated allantois. The amnion is thin and smooth. (**E**) Representative stage-matched *Smad5*$^{m1/m1}$ (KO) littermate with abnormal body curvature, underdeveloped anterior structures and foregut, vestigial heart, broad base of the allantois and an aggregate on the amnion (*). (**F**) Number of PGCs detected in embryos of the three *Smad5* genotypes at late streak, neural plate and headfold stages. Wilcoxon's summed ranks test was used for statistical analysis (***, P<0.001; **, P<0.01; *, P<0.05), and medians are depicted by a bar. (**G**,**H**) Dorsal view of wild-type (28S) and *Smad5*$^{m1/m1}$ (26S) mutant embryos dissected free from their yolk sac. The amnion is a thin, smooth membrane that envelops the embryo (G, arrowheads). A characteristic aggregate of cells is present on the mutant amnion (H, arrow). (**I**) Whole-mount staining for alkaline phosphatase (AP) activity in a mutant amnion (10-11S stage) with an aggregate of cells. A cluster of ectopic AP^{+} (brown; arrow) PGC-like cells projects from the ectoderm side of the amnion. (**J**) AP staining of a section through the aggregate of cells on the mutant *Smad5*$^{m1/m1}$ amnion shown in H, at the level of the hindbrain. Ectopic PGC-like cells (red) are localized in close association with the amnion ectoderm. Scale bars: 500 μm in G,H; 200 μm in K; 100 μm in C,D,J. Al, allantois; Am, amnion; AmEc, amnion ectoderm; AmMe, amnion mesoderm; EHF, early headfold; He, heart; Hf, headfold; Hg, hindgut; LNP, late neural plate; LS, late streak; NP, neural plate; Nt, neural tissue.

until the late neural plate (LNP) stage. There was negligible extension between the LNP and 1-2 somite (S) stage, but cellular material accumulated into the base of the allantois, expanding its width (Fig. 1B) and producing irregularities. Normal extension was resumed after the 1/2S stage until fusion with the chorion at ~6S stage, which occurred in most mutants with an irregularly shaped and short allantois (Fig. 1A,B,D,E). Initiation of the allantois was also delayed in the heterozygotes at LS stages (P<0.01) (Fig. 1A); extension was then parallel to that of the wild type until chorion-allantoic fusion. This phenotype is very similar to that in *Bmp4* heterozygotes (see Fig. S1A in the supplementary material). The delay in allantoic initiation and the later growth defect in the *Smad5* mutant are not due to general growth retardation, as shown by relating allantois length to embryonic axis length (Fig. 1C, Fig. S1B): the differences remained.

At the HF stage, the amnion is a thin membrane composed of two layers of squamous epithelium: the amnion ectoderm is continuous with the embryonic surface ectoderm and the amnion mesoderm is continuous with the yolk sac mesoderm and, posteriorly, with the allantois mesothelium. The two layers are derived from slightly different regions of the early-streak stage epiblast (Lawson et al., 1991) (K.A.L., unpublished). The amnion was markedly thickened in *Smad5*$^{m1/m1}$ embryos (Table 1). The amnion of somite-stage mutants typically contained aggregates of cells (Table 1) that were often localized very anteriorly at a remote distance from the allantois. From the 5S stage onwards, *Smad5*$^{m1/m1}$ embryos had an underdeveloped forebrain and heart when compared with stage-matched control littermates, and an aggregate of cells was visible on the amnion in more than half of the mutants (Fig. 1D,E). Failure of embryo turning, defects in heart looping and dilation of embryonic and yolk sac blood vessels were as previously described (Chang et al., 1999; Chang et al., 2000).

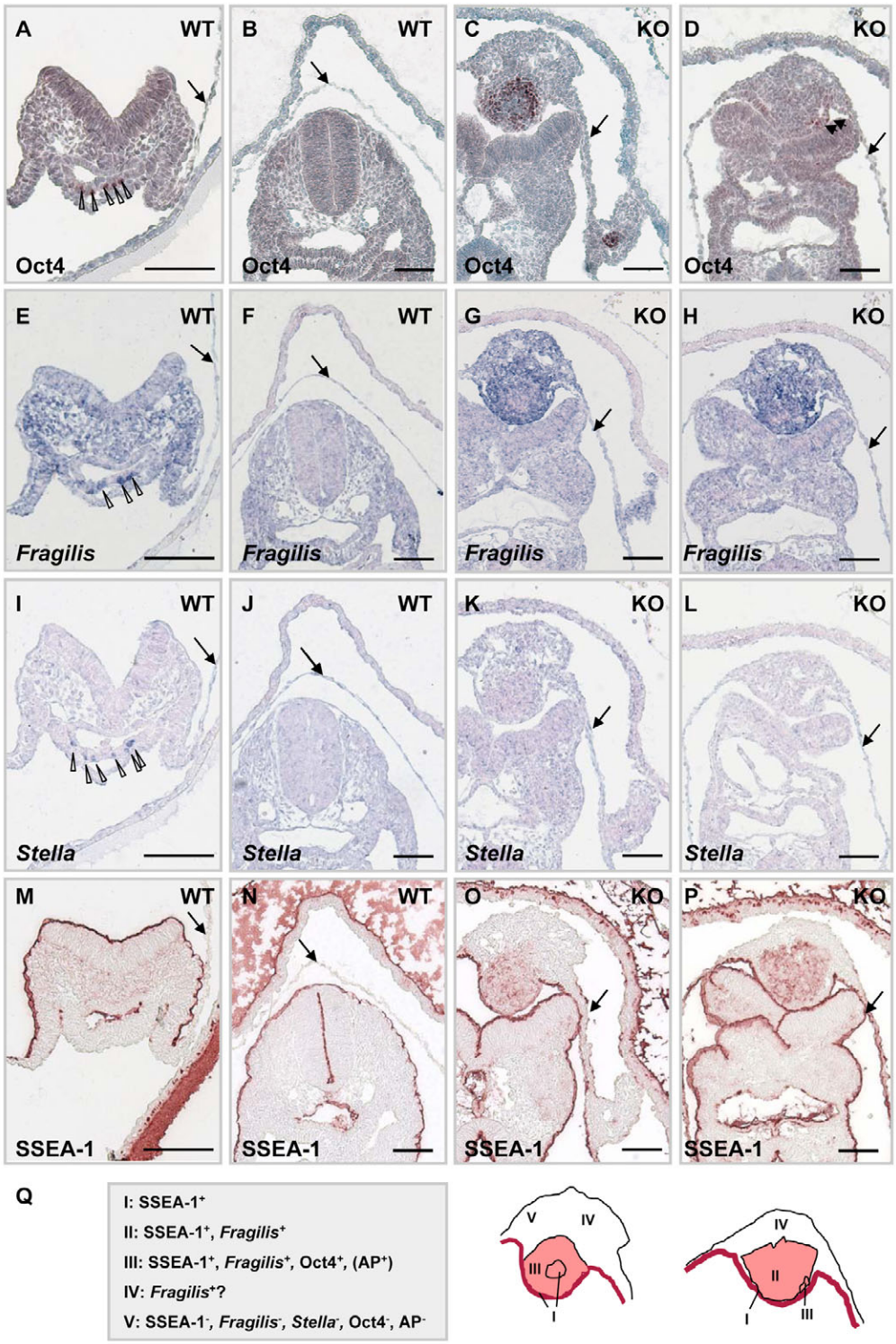

Fig. 2. Epiblast/stem cell and PGC-markers in *Smad5*$^{m1/m1}$ embryos. Transverse sister sections through hindgut region (A,E,I,M) and head region (B,F,J,N) of an E8.5 wild-type embryo, and of an E8.5 *Smad5*$^{m1/m1}$ littermate with multiple aggregates of cells on the amnion (C,D,G,H,K,L,O,P). The arrow points to the amnion. (**A-D**) Anti-Oct4 antibody staining demonstrates the presence of PGCs in the hindgut (A; open arrowheads). Oct4$^+$ cells are absent in control (B) and non-thickened mutant amnion (C,D). Ectopic Oct4$^+$ cells can be observed regionally in some aggregates in mutant amnion. Oct4$^+$ cells have an ectoderm oriented localization (C,D). (**E-H**) PGCs in the hindgut are marked by their fragilis expression (E; open arrowheads). Ectopic fragilis$^+$ cells can be observed within the aggregate of mutant amnion, but not in the non-thickened amnion (G,H). (**I-L**) *Stella* is expressed in PGCs in the hindgut (I; open arrowheads). *Stella* expression was never observed in wild-type (J) or mutant (K,L) amnion, also not in regions where Oct4$^+$, SSEA-1$^+$ and fragilis$^+$ cells are residing (K,L). (**M-P**) Anti-SSEA-1 antibody staining demonstrates the presence of SSEA-1 in surface ectoderm, visceral endoderm and the neuroectoderm (N). At this stage of development PGCs in the hindgut are SSEA-1 negative (M). There is intense SSEA-1 staining in the mutant amnion ectoderm, and weaker staining can be observed in the aggregates. (**Q**) Schematic representation of the different regions that can be recognized within the mutant amnion. Scale bars: 100 μm.

DEVELOPMENT

De-novo appearance of AP-positive cells in the Smad5 mutant amnion

Chang and Matzuk (Chang and Matzuk, 2001) described a *Smad5* gene dosage effect, reminiscent of, although less pronounced than, the *Bmp4* null allele, on the size of the PGC founder population in a 129SvEv/C57 mixed genetic background. We confirm these observations now in the C57BL/6J and F2 background (see Fig. S2 in the supplementary material), and have determined that the incidence and number of PGCs is already reduced in *Smad5* mutants at the LS stages, with an intermediate effect in the heterozygotes (Fig. 1F). Chang and Matzuk (Chang and Matzuk, 2001) observed AP- and Oct4$^+$ cells in the aggregate of cells in the amnion of early somite-stage embryos, and concluded that they are mislocated PGCs. We explored the timing of appearance of these PGC-like cells in the amnion. Although half of the NP up to the 4S stage embryos had defects in allantois development, amnion closure and amnion thickening, no AP$^+$ PGC-like cells were seen in the *Smad5*$^{m1/m1}$ amnion at these stages (Table 1), or elsewhere outside the normal PGC domain. Only after the 5S stage, did we find AP$^+$ cells in some of the distinct aggregates of cells on the anmion (Fig. 1H,I,J; Table 1). These were located in the part of the aggregate projecting into the amniotic cavity and therefore associated with amnion ectoderm (Fig. 1J), unlike the ectopic haematopoietic and endothelial cells that bulged into the mesoderm side of the amnion facing the exocoelom. By contrast to previous data (Chang and Matzuk, 2001), we found that AP$^+$ clumps were still prominent at E9.5 (11/14 embryos: 16-28S) (Fig. 1H,J; Table 1). The sudden appearance of PGC-like cells in appreciable numbers in the aggregates (33 to 119 PGC-like cells in 5S-12S embryos; 142 cells in the aggregate of the 26S mutant shown in Fig. 1H,J), and the anterior position of the aggregates containing them, make it unlikely that they are PGCs mislocated from the founder population, and supports the argument for a change in cell fate in situ in the mutant amnion.

The AP$^+$ cells in the *Smad5* mutant amnion are not bona fide PGCs

We used a panel of markers to address the possibility that the AP$^+$ cells in the aggregates were de-novo induced PGCs. The epiblast expresses *Oct4*. During gastrulation the expression of *Oct4* is downregulated and is thereafter only maintained in the germ cell lineage (Schöler, 1991) (Fig. 2A). Wild-type and non-affected *Smad5*$^{m1/m1}$ amnion was always devoid of Oct4 protein (Fig. 2B-D), but the cell aggregates often contained Oct4$^+$ cells (Fig. 2C,D). At E6.5, fragilis (Ifitm3/Mil1) is expressed in proximal epiblast (Saitou et al., 2002), the region in which PGC-competent cells reside (Lawson and Hage, 1994). During gastrulation, fragilis expression increases within a cluster of cells at the base of the allantoic bud. At E7.5 (early bud stage) cells with the highest expression of fragilis initiate at the germ cell-characteristic expression of *Stella/PGC-7/Dppa3* (Saitou et al., 2002; Tanaka et al., 2004; Tanaka et al., 2005). Fragilis expression level in non-thickened amnion was comparable to wild-type amnion. In the aggregate, an ectopic fragilis expression domain was observed that contained Oct4$^+$ cells, but exceeded this domain (Fig. 2G,H, compared with 2C,D). Although we observed *Stella*-expressing PGCs in the hindgut of wild-type and *Smad5*$^{m1/m1}$ embryos (Fig. 2I, data not shown), we did not find any *Stella*-expressing cell in the cell aggregates in the *Smad5*$^{m1/m1}$ amnion (Fig. 2K,L, data not shown).

Mouse SSEA-1 is expressed in epiblast, postgastrulation ectoderm and endoderm, and in migrating PGCs (Fox et al., 1981). We detected expression in visceral and gut endoderm, and in surface ectoderm (Fig. 2M,N), but at E8.5, PGCs in the hindgut were still SSEA-1 negative (Fig. 2M) (Donovan et al., 1986). Remarkably, *Smad5*$^{m1/m1}$ embryos had a robust SSEA-1 staining throughout the entire ectoderm, and sporadically also in the mesoderm, of the bilayered amnion (Fig. 2N,O). In addition, we observed that SSEA-1$^+$ regions largely overlapped with fragilis$^+$ cells of the aggregate (Fig. 2N,O).

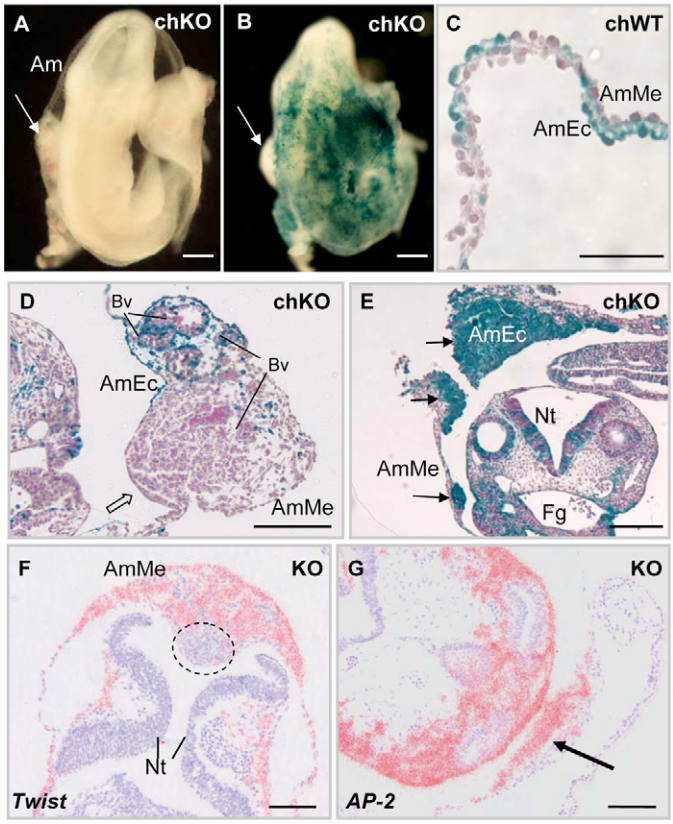

Fig. 3. Perturbed homeostasis in the mesoderm and ectoderm component of the amnion in *Smad5*$^{m1/m1}$→WT^{lacZ} and *Smad5*$^{m1/m1}$ embryos. (**A**,**B**) Dorsal view of a low-percentage E9.5 *Smad5*$^{m1/m1}$→WT^{lacZ} chimeric embryo, unstained (A) and stained for β-galactosidase activity (B). The head is patterned normally and the headfolds and neural tube are closed, but embryonic turning is mildly affected (a twisted tail). The amnion remains locally thickened (white arrow), and red blood cells can be observed within this aggregate of cells (A; open arrowhead). (**C-E**) Section through low-percentage control *Smad5*$^{+/m1}$→WT^{lacZ} (chWT) (C) and *Smad5*$^{m1/m1}$→WT^{lacZ} chimeras (chKO) (D-E). *Smad5*$^{+/m1}$ and *Smad5*$^{m1/m1}$ ES cell derivatives colonize both the mesoderm and ectoderm of the amnion extensively (E). Aggregates of cells on the amnion are of mixed wild type (blue) and *Smad5*$^{m1/m1}$ (purple) origin in a *Smad5*$^{m1/m1}$→WT^{lacZ} chimera (D). The amnion ectoderm is cuboidal in one part of the aggregate of cells (open arrow). Blood vessels develop always in the mesodermal side of the aggregate. In another *Smad5*$^{m1/m1}$→WT^{lacZ} embryo the amnion ectoderm is completely of wild-type origin (E). (**F**) *Twist* is expressed in amnion mesoderm, including in the clump of cells in *Smad5*$^{m1/m1}$ mutant amnion, but *Twist*^{neg} areas can also be distinguished (dashed circle). (**G**) Thickened, *AP-2*$^+$ amnion ectoderm is observed locally in a clump of cells (arrow) in a *Smad5*$^{m1/m1}$ mutant amnion. Al, allantois; Am, amnion; AmEc, amnion ectoderm; AmMe, amnion mesoderm; Bv, blood vessel; Ex, extraembryonic region; Fg, foregut; He, heart; Hf, headfold; Nt, neural tissue; Op, optic anlage; So, somite; Ys, yolk sac. Scale bars: 100 μm in A, E-G; 50 μm in B-D.

DEVELOPMENT

Based on this marker analysis we identified several distinct areas in *Smad5*$^{m1/m1}$ mutant amnion (Fig. 2Q): (1) SSEA-1$^+$ amnion with normal appearance resembling surface ectoderm; (2) SSEA-1$^+$ and fragilis$^+$ areas in the cell aggregates, and within these areas; (3) SSEA-1$^+$, fragilis$^+$, Oct4$^+$, AP$^+$ cells that did not express *Stella*. Further co-localization and marker studies may rule out whether cells exist that are either SSEA-1$^+$ or fragilis$^+$, and unravel the precise provenance and identity of the cells. The absence of *Stella* expression rules out the possibility that the AP+ cells are fully specified PGCs; the expression pattern found is compatible with reversion by the mutant amnion to a pluripotent state. At the mesodermal side of the aggregate facing the exocoelom, cells could be detected that did not express any of the PGC/epiblast/ES cell markers.

Smad5 is essential for both cell layers of the amnion to preserve homeostasis

Chimeric embryos offer the possibility of analysing interactions between normal and mutant cells. Although the majority of the *Smad5*$^{m1/m1}$→WT^{lacZ} chimeras (14 out of 18) of *Smad5*$^{m1/m1}$ ES cells in wild-type *lacZ* transgenic (WT^{lacZ}) host embryos were high chimeras with >90% mutant cells in the epiblast derived tissues, the low-percentage chimeras (estimated between 20 and 80% chimerism, depending on the embryo) were very instructive. They had the typical mutant phenotype in the extra-embryonic tissues, with large cell aggregates in the amnion (Fig. 3A,B). *Smad5*$^{m1/m1}$ cells made, just like descendants from wild-type ES cells (Fig. 3C), an unbiased contribution to the mesodermal and ectodermal components of the amnion (Fig. 3D,E). Intriguingly, the aggregates in low-percentage chimeras were not composed solely of disorganized mesodermal cells, which we anticipated from our earlier work (Chang et al., 1999), but the amnion ectoderm was also sometimes thickened, and was even entirely of wild-type origin in one chimera (Fig. 3E). This suggests that loss of Smad5 in the mesoderm affects not only the mesodermal but also the ectodermal component of the amnion, and attributes a non-cell-autonomous function to Smad5 in mesoderm. Based on this result, we re-evaluated the expression of *Twist* (amnion mesoderm) and *AP-2* (amnion ectoderm) in *Smad5*$^{m1/m1}$ amnion. Aggregates of cells are predominantly of mesodermal origin but sometimes contain locally a thickened *Twist* negative and *AP-2* positive ectodermal component (Fig. 3F,G).

Loss of *Smad5* leads to an increase in expression of Bmp genes and Bmp target genes in the amnion

The expansion of the amnion may result from a change in either cell proliferation or cell shape from a columnar or cuboidal to an extreme squamous morphology. Bmp2 has been implicated in amniotic expansion, but the mechanisms remain elusive (Zhang and Bradley,

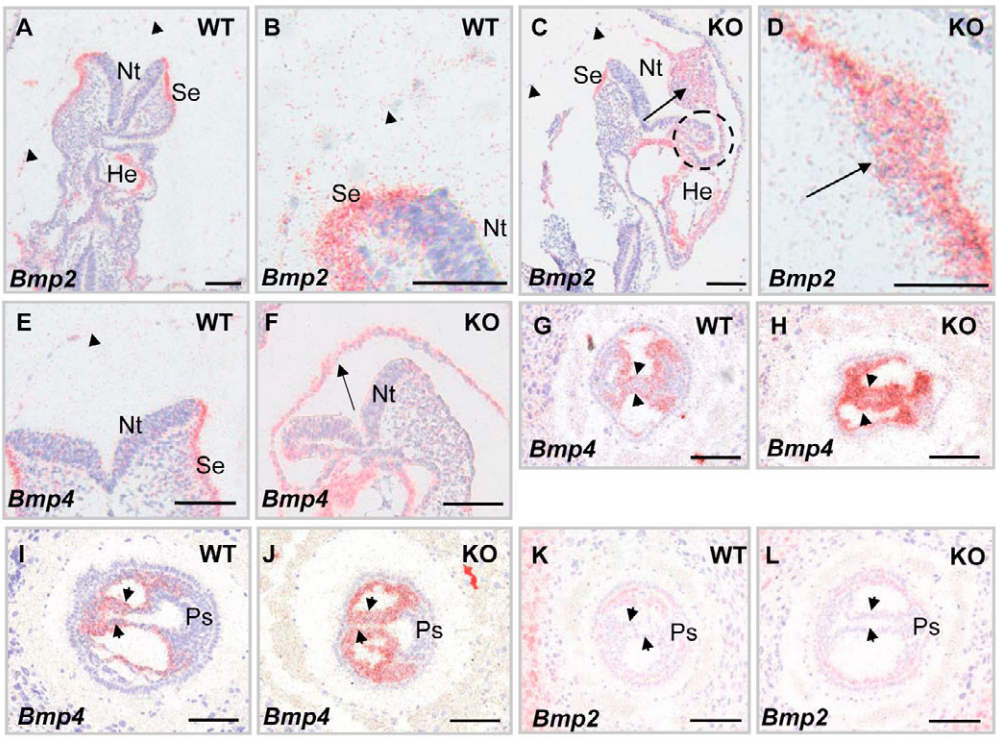

Fig. 4. Ectopic expression of *Bmps* in *Smad5*$^{m1/m1}$ amnion. (**A-F**) Ectopic expression of *Bmp2* and *Bmp4* in mutant amnion at E8.5. Compared with the wild-type littermate (A,B), the expression of *Bmp2* is highly elevated in the aggregate of cells (KO, arrow) and the flanking mutant amnion, but not in more remote squamous amnion (arrowhead) (C,D), or in surface ectoderm. *Smad5* $^{m1/m1}$ embryos express much higher levels of *Bmp4* throughout the amnion (F), than do controls (E). *Bmp4* expression levels appear weaker in mutant surface ectoderm (E,F). Surface ectoderm and amnion ectoderm are often poorly delineated in *Smad5* $^{m1/m1}$ embryos when the aggregate of cells on the amnion is localized anteriorly (dashed circle; C). (**G-L**) Enhanced expression of *Bmp4*, but not of *Bmp2*, in mutant amnion at E7.0. *Bmp4* is expressed in wild-type amnion at EB and NP stages, respectively (G,I), but its expression is elevated in the amnion of mutant littermates (H,J). The *Bmp2* expression is not yet significantly different in the amnion of wild-type (K) and mutant (L) EB littermates. Short arrows point towards the mesodermal component of the amnion, and are positioned in the exocoelom. Anterior is to the left and posterior to the right. AmMe, amnion mesoderm; He, heart; Nt, neural tube; Ps, primitive streak; Se, surface ectoderm; Ys, yolk sac. Scale bars: 100 μm in B-H,J,L; 50 μm in A,I,K.

DEVELOPMENT

1996). We evaluated the expression of *Bmp* genes, and some of their target genes and modulators. *Bmp2* transcript levels were extremely low in the wild-type amnion at E8.5, if at all above background (Fig. 4A,B), whereas *Bmp4* expression was detectable in amnion (Fig. 4E). A dramatic increase of *Bmp2* and *Bmp4* transcripts was observed in the *Smad5*$^{m1/m1}$ amnion. *Bmp2* was upregulated in the cells of the aggregates and neighbouring unaffected amnion, but not in squamous amnion distant from the aggregate (Fig. 4C,D). *Bmp4* was significantly upregulated, also in squamous amnion (Fig. 4F), but the expression of *Bmp7* appeared unaffected (data not shown). During gastrulation, *Bmp4* expression is dynamic. Expression persists within the extra-embryonic ectoderm, and *Bmp4* transcripts become detectable in the extra-embryonic mesodermal components of the amniotic folds, and subsequently in the amnion, yolk sac and chorion that line the exocoelom, as well as within the allantoic bud/allantois (Lawson et al., 1999) (data not shown). At the NP stage, before detectable thickening of the mutant amnion, *Bmp4* levels appeared already more robust in the amnion of mutants when compared with control littermates (Fig. 4G-J). *Bmp2* expression was low at this stage of amnion development, without clear differences between mutants and controls (Fig. 4K,L).

The observed upregulation of *Bmp2/4* may cause increased Bmp signalling via Smad1/8 or non-Smad pathways, including ERK1/2 (Nakamura et al., 1999; Qi et al., 2004). The pattern of phosphorylated (P)-ERK1/2 staining at E7.5 and 8.5 in wild-type littermates is very variable and reflects the dynamic nature of phosphorylation-dependent signalling cascades (data not shown). At E7.5 and 8.5 P-ERK1/2-positive cells are very rare in the wild-type amnion (Fig. 5A, data not shown). No dramatic increase in P-ERK1/2 staining was observed in non-thickened amnion (Fig. 5B,C, data not shown); however, manifest ERK signalling was observed within the aggregates. Likewise, the P-Smad1/5/8 staining pattern was very dynamic in E7.5 and 8.5 wild-type littermates, and could be observed only sporadically in amnion (Fig. 5D). In the *Smad5*$^{m1/m1}$ amnion enhanced P-Smad1/8 staining was most evident in the aggregate (Fig. 5E,F). These results illustrate enhanced Bmp signalling in the mutant amnion.

We then analysed the expression of acknowledged Bmp target genes in the *Smad5*$^{m1/m1}$ amnion. Periostin*/Osf2* is involved in cell adhesion and spreading (Kruzynska-Frejtag et al., 2001), and at E8.5 its only sites of expression are the amnion and the yolk sac (Fig. 5G). In the *Smad5*$^{m1/m1}$ amnion, periostin expression was more pronounced, although excluded from the aggregate of cells (Fig. 5H). *Msx2* is expressed in surface ectoderm (Monaghan, 1991) but barely in amnion (Fig. 5I). *Msx2* is robustly expressed in the mutant amnion, predominantly in its ectodermal component (Fig. 5J). This shows that higher *Bmp2/4* levels indeed result in increased expression of Bmp target genes in the *Smad5*$^{m1/m1}$ amnion. Genes

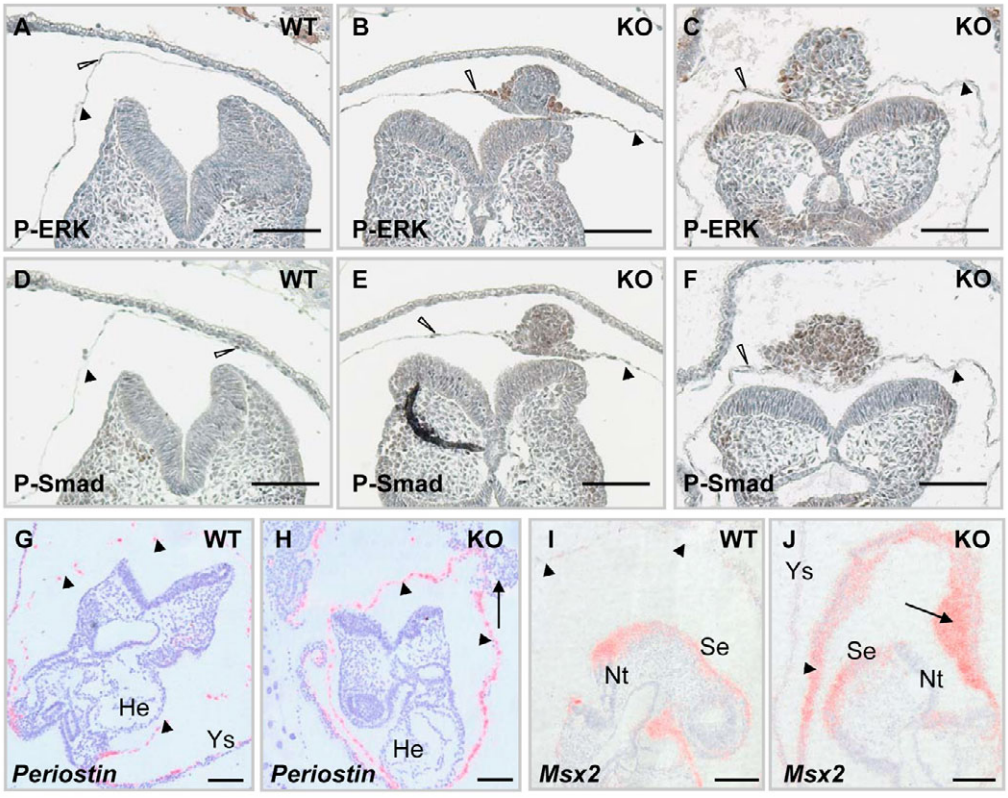

Fig. 5. Ectopic Bmp signalling in *Smad5*$^{m1/m1}$ amnion. (**A-C**) Anti-P-ERK1/2 antibody staining can barely be detected in the amnion (arrowhead) at E8.5 (A). It is increased in non-thickened *Smad5* mutant amnion but especially elevated in the aggregate of cells (B,C). B and C represent two different Smad5 mutants. (**D-F**) Anti-phospho-Smad1/5/8 antibody staining can only be detected sporadically in an isolated cell of the amnion (arrowhead) at E8.5 (A). P-Smad1/5/8 is upregulated in non-thickened mutant amnion and within the aggregates of Smad5 mutant amnion. Sections in D-F are sister sections of A-C. (**G**,**H**) The Bmp target gene periostin is expressed in the amnion (arrowhead) at E8.5. It is strongly upregulated in the non-thickened *Smad5* mutant amnion, although excluded from the aggregate of cells (H). (**I**,**J**) The Bmp target gene *Msx2* is barely detectable in wild-type amnion (I) but highly expressed in mutant amnion at E8.5 (J). *Msx2* expression is primarily confined to the ectodermal component of the amnion (arrowhead) and the aggregate of cells (arrow). The expression of *Msx2* in the embryo proper is not altered significantly. AmMe, amnion mesoderm; He, heart; Nt, neural tube; Se, surface ectoderm; Ys, yolk sac. Scale bars: 100 μm.

encoding Bmp antagonists like noggin, chordin and *Smad7* are expressed at low levels in the amnion and no significant changes in their expression domain were detected in *Smad5*$^{m1/m1}$ embryos (data not shown).

Administration of BMP4 can mimic the early Smad5 deficiency amnion defect

The ectopic expression of *Bmp2* and *Bmp4*, and of several Bmp target genes, as well as the different Bmp-sensitive cell types that arise in a regionalized fashion in the *Smad5* mutant amnion, favours a gain-of-Bmp-function model underlying the *Smad5*$^{m1/m1}$ amnion defect. To test this hypothesis, we injected recombinant mature BMP4 (rBMP4) in the exocoelom of NP- to HF-stage wild-type embryos, and cultured these whole embryos until early somite to 10-15S stages, when the amnion was then screened for the presence of cell aggregates. Small clumps of cells were observed sporadically in embryos injected with rBMP4 (2/10 NP, 6/25 EHF to HF stages), whereas control-injected embryos never developed a similar defect (0/10 NP, 0/15 EHF to HF) (Fig. 6A-F). The aggregates were sometimes only recognizable after histological analysis. These results show that even in a wild-type context, excess BMP4 can induce thickening of the amnion, confirming that BMP levels are crucial for preserving amnion homeostasis.

DISCUSSION

Smad5 in extra-embryonic development

Smad5 is essential for PGC development and for correct extra-embryonic development, including the development of the allantois and the amnion. We can now order the appearance of these defects in the Smad5-deficient proximal epiblast and its extra-embryonic descendants as follows: (1) delayed appearance of the allantois, presumably associated with the reduced PGC founder population in *Smad5* mutants (both evident at the LSEB stage); (2) a relative posterior and delayed closure of the amnion visible in LSEB to HF stages, and abnormal morphogenesis of the allantois after the LNP stage; (3) anterior defects involving the delineation between anterior neural plate and ectoderm, including the amnion ectoderm (first identifiable at NP and EHF stages), and a thickened amnion at HF stages; and (4) distinct aggregates of cells on the amnion of early somite embryos, which become vascularized and haematopoietic, and often contain Oct4^{+} and AP^{+} cells from 5S stage onwards.

The delay in allantoic bud formation in *Smad5* mutants, and the reduced incidence and number of PGCs at the LSEB stage, reflects a well documented loss of Bmp signalling effect initiated in the extra-embryonic ectoderm and visceral endoderm (reviewed by Zhao, 2003). The relatively short allantois in *Smad5* heterozygotes, and in *Bmp4* heterozygotes, is a consequence of the slight delay in allantois initiation, rather than an effect on cell recruitment to, and proliferation in, the bud. Absence of Smad5 results in abnormal morphogenesis of the allantois after delayed initiation and early normal extension. Failure to extend further during the rest of the cell recruitment and proliferation phases (Downs and Bertler, 2000), and the accumulation of material in the base of the allantois, suggest that cell redistribution may be more affected than the addition of cells. The resumption of extension after the 2S stage coincides with the normal end of recruitment and rapid proliferation and the onset of extension by cavitation and vascularization (Downs and Bertler, 2000). This process appears to be Smad5-independent or open to functional compensation, presumably by *Smad1* or *Smad8*. These latter Bmp-Smads are also expressed in the amnion and allantois (Tremblay et al., 2001; Hayashi et al., 2002) and could implement its closure, the delay of which is probably caused by reduced Bmp2 signalling during an earlier phase of amnion development (Zhang and Bradley, 1996).

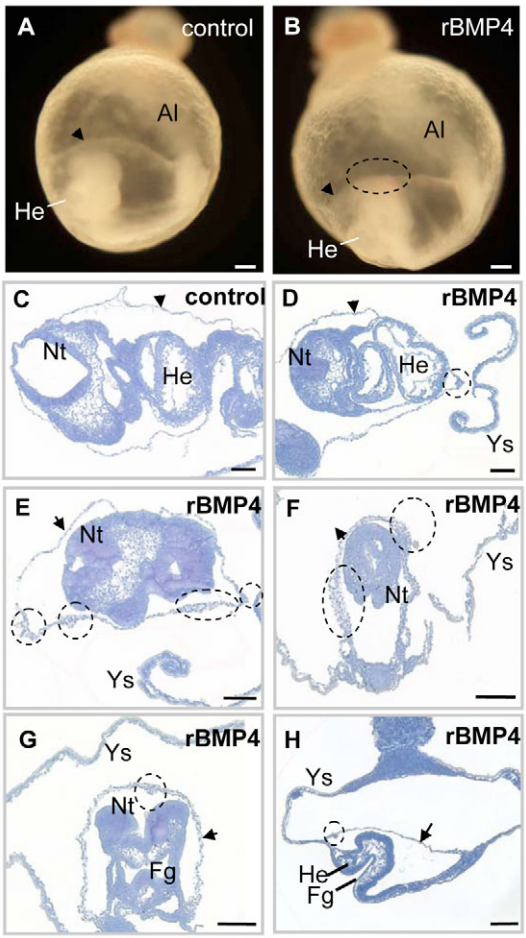

Fig. 6. Local administration of rBMP4 induces thickening of the amnion in wild-type embryos. (**A**,**B**). Lateral view of wild-type embryos that were either control injected (A) or injected with rBMP4 (B) in the exocoelom at the EHF stage (E7.5), and cultured in vitro until the 5S stage. The amnion (arrowhead) developed a local thickening in the rBMP4-injected embryo (dashed circle). Aggregates were always much smaller than in *Smad5* mutants, and difficult to see through the yolk sac. (C-F) Sections through control (**C**) and rBMP4-injected (**D-H**) embryos. The appearance and size of the amnion thickening (dashed circle) varied significantly between embryos. Thickening of the amnion was only scored when observed in more than five successive sections. The embryos in C-E were injected at the HF stage; D and E are sections from the same embryo, illustrating that amnion thickening can develop at different locations. The embryos in F-H were injected at the NP stage. The embryo in H has an unusually large yolk sac. Al, allantois; Fg, foregut; He, heart; Nt, neural tissue; Ys, yolk sac. Scale bars: 100 μm.

A more striking *Smad5*$^{m1/m1}$ defect is the ectopic vasculogenesis, haematopoiesis and development of Oct4^{+} and AP^{+} cells that can be observed in the aggregate of cells in the *Smad5*$^{m1/m1}$ amnion. Previously, we proposed an exclusive mesodermal origin for these aggregates of cells (Chang et al., 1999). New evidence from the low-percentage chimeras showed that the aggregates are not exclusively comprised of mesodermal cells but occasionally also contain thickened ectoderm. The mesodermal part of the aggregates in mutants can result from

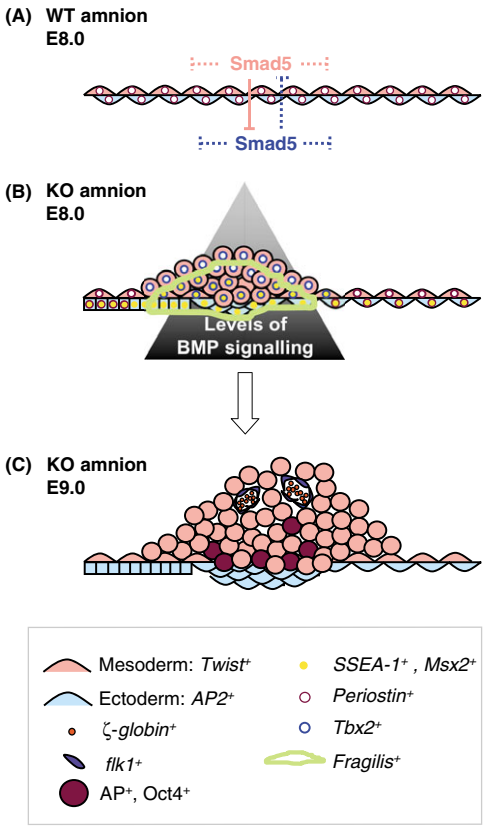

Fig. 7. Model for the role of Smad5 signalling in amnion homeostasis. (**A**) The squamous, bilayered wild-type amnion at the early somite stage is composed of a mesoderm layer facing the exocoelom that expresses *Twist*, whereas an epithelial cell layer that expresses *AP-2* lines the amniotic cavity. The chimera analysis demonstrates that Smad5 is essential in the mesoderm, where it functions in a non-cell-autonomous fashion, because mutant mesoderm cells can elicit thickening of wild-type amnion ectoderm. Reciprocally, however, we cannot conclude that Smad5 functions also non-cell-autonomously and/or cell autonomously in the ectoderm. (**B**) At the early somite stage the *Smad5*$^{m1/m1}$ mutant amnion displays an altered cellular organization with a zone of primarily thickened mesoderm but also thickened ectoderm. The mutant amnion ectoderm is positive for SSEA-1. The anterior amnion ectoderm remains cuboidal (squares), and is in continuity with anterior surface ectoderm and anterior neural tissue. Robust ectopic expression of *Bmp2* and *Bmp4* in mutant amnion is associated with increased Smad1/8 and ERK1/2 signalling and expression of periostin, *Tbx2,* fragilis and *Msx2*. The differential but overlapping ectopic expression patterns of all these Bmp-target genes suggest that cells in the mutant amnion sense different levels of Bmp signalling. How these different levels of Bmp signalling are established in the mutant amnion remains to be explored. (**C**) The transformation of the amnion to a complex tissue with different Bmp-sensitive cell types, such as e.g. an Oct4$^+$, AP$^+$, SSEA-1$^+$ and fragilis$^+$ region reminiscent of PGC-competent epiblast, *Flk1*-expressing endothelial cells and ζ-globin-expressing cells (see Discussion). The ectopic and appreciable numbers of AP$^+$ cells arise suddenly from the 5S stage onwards, which argues strongly for their in situ change in fate. The AP$^+$ cells are localized near the ectodermal component of the aggregate, whereas haematopoietic and endothelial cells are positioned at the exocoelomic side. Our data suggest that Smad5 is the predominant Bmp signal-mediator in the amnion, and controls Bmp expression levels and amnion homeostasis tightly. Upon Smad5 removal the control of *Bmp* expression is released, which results in an excess of Bmp, in take-over by non-Smad5 pathways and ultimately in gain of Bmp signalling defects.

altered proliferation, disorganization or misdifferentiation of amniotic mesoderm cells, and/or from the previously proposed mislocation of allantois tissue (Chang et al., 1999). These aggregates are remarkably often localized very anteriorly, at a remote distance from the allantois, but the mesoderm in the aggregates expresses *Tbx2* that is also expressed by allantois tissue (Chang et al., 1999). However, in the murine allantois vasculogenesis occurs without haematopoiesis (Downs et al., 1998), whereas the *Smad5* mutant amnion contains not only *flk-1* expressing endothelial cells, but also ζ-globin-expressing primitive blood cells (Chang et al., 1999). Hence, the amnion adopts allantois and blood island-like fates in the absence of Smad5.

Addressing allantois mislocation versus amnion misdifferentiation remains elusive by marker gene analysis, but here our PGC study is instrumental. Although defects in amnion and allantois development can be detected as early as the NP stage, ectopic AP$^+$ cells were never found in thickened *Smad5*$^{m1/m1}$ amnion before the 5S stage. After the 5S stage the majority of the *Smad5*$^{m1/m1}$ embryos had aggregates of cells on the amnion, of which half contained an appreciable number of AP$^+$ and Oct4$^+$ cells. This late appearance of AP$^+$ cells in *Smad5* mutants is in contrast to the ectopic PGCs that can be readily distinguished in the yolk sac of *Otx2* and *Smad2* mutants, and in extra-embryonic mesoderm of tetraploid *Bmp4* chimeras at HF and early somite stages (K.A.L., unpublished) (Tremblay et al., 2001; Fujiwara et al., 2001). Therefore, it is very unlikely that AP$^+$ cells are swept into ectopic locations immediately after PGC allocation at ~E7.2 in *Smad5*$^{m1/m1}$ embryos and remain unrecognized. Our analysis is suggestive of an in situ change in fate of amnion cells.

The AP$^+$ cells are unlikely to be de-novo induced, bona fide PGCs because no *Stella*-expressing cells were ever observed in the aggregates. Although the coexpression of AP, Oct4, and SSEA-1 could indicate the presence of pluripotent, ES-like cells, the combination of AP, Oct4, SSEA-1 and fragilis expression is more reminiscent of an earlier developmental state; PGC-competent epiblast. Fragilis is a direct target gene of extra-embryonic-derived Bmp4 in the PGC-competent epiblast (Saitou et al., 2002). The ectoderm of non-affected *Smad5* mutant amnion has characteristics of surface ectoderm (SSEA-1$^+$ and *Msx2*$^+$). Despite this reminiscence of surface ectoderm, the amnion ectoderm expresses also periostin, a gene normally not expressed in surface ectoderm.

Remarkably, when isolated human amnion membrane cells are cultured, they also express *Oct4* and the epiblast/stem cell/PGC marker *Nanog* (Miki et al., 2005). These isolated human cells have the potential to differentiate to all three germ layers – endoderm (hepatocytes), mesoderm (cardiomyocyte) and ectoderm (neural cells) – in vitro (Sakuragawa et al., 2004; Tamagawa et al., 2004; Zhao et al., 2005).

Smad5 deficiency results in gain-of-Bmp-function defects

The *Smad5*$^{m1/m1}$ amnion defect is accompanied by a specific and robust upregulation of *Bmp2* and *Bmp4*, whereas the expression of *Bmp7* appears unaffected. This suggests that Smad5 is normally a predominant Bmp-Smad in the amnion that, directly or indirectly, negatively regulates *Bmp2/4* expression. Ectopic *Bmp4* expression is readily visible before local thickening of the amnion at the LSEB stage, and subsequently in the aggregate of cells, but also in the neighbouring, seemingly unaffected amnion.

The mutant amnion displays elevated Smad-dependent (Bmp-regulated phospho-Smad1/5/8) and Smad-independent (P-ERK1/2) signalling. Enhanced Bmp signalling is also demonstrated by alterations in the expression pattern of target genes of Bmp. A patent upregulation of periostin can be appreciated in seemingly unaffected mutant amniotic cells. *Tbx2* (Chang et al., 1999), fragilis and *Msx2* are, unlike periostin, highly upregulated in the aggregate of cells in the mutant amnion. *Msx2* is predominantly expressed in the ectoderm component of the aggregate and non-thickened amnion. The increased or ectopic expression of these Bmp target genes in distinct but overlapping domains may indicate that expression of these target genes requires different dose windows of (combined) Bmp(s), which is reminiscent of the different doses of Bmp4 signalling that are required for dorsoventral patterning of mesoderm in *Xenopus* embryos (Dosch et al., 1997). A localized source of ligand(s) or antagonists/modulators, or several sources of ligands (e.g. Bmp2 and Bmp4) could establish graded signalling. Alternatively or additionally, differences in presence and concentration of signalling components, but also unexplored endogenous differences in affinities of Smad1, and Smad8 and non-Smad cascades to activated receptors, Smad-interacting proteins and their shared target genes, will determine the outcome of Smad5 deficiency in different regions of the amnion.

The *Smad5*$^{m1/m1}$ amnion acquires features of different Bmp-sensitive lineages, such as allantois and blood island tissue but also PGC-competent epiblast (Lawson et al., 1999) (reviewed by Zhao, 2003; Fujiwara et al., 2001). In the mutant amnion, epiblast-like cells are localized near the ectodermal component, whereas ectopic endothelial and haematopoietic cells are positioned at the exocoelomic side of the aggregate. Concurrent with the differential ectopic expression patterns of several Bmp target genes, this regionalization of the aggregates makes it conceivable that cells indeed interpret different levels of Bmp signalling – whether quantitative and/or qualitative – that determine their subsequent fate (Fig. 7). Bmp4 is not only implicated in differentiation of different cell lineages, but it is also pivotal in maintaining self-renewal of ES cells (Ying et al., 2003; Qi et al., 2004).

Our gain-of-Bmp-function model is especially challenging, as no other mutant mouse model of a Bmp signalling component has been associated so far with ectopic vasculogenesis, haematopoiesis and development of (PGC-competent) epiblast-like cells in the amnion. Evidence that gain of Bmp function may indeed underlie the *Smad5* mutant amnion phenotype comes from the induction of amnion thickening in wild-type amnion when rBMP4 is topically administered. Single injection of rBMP4 in the exocoelom compared to constitutive secretion of Bmp4 and Bmp2 in *Smad5* mutants is just one out of many explanations why clumps could be significantly smaller in rBMP4-injected embryos than in mutants. The converse experiment, in which *Smad5*$^{m1/m1}$ embryos would be rescued by injecting Bmp antagonists such as Noggin and/or Chordin, is appealing. However, it is far more complicated to accomplish, as systemic administration of excess amounts of antagonists would be required to neutralize endogenous Bmps.

Our study has revealed novel aspects of Smad5 signalling, i.e. a non-cell-autonomous function for Smad5 in amnion mesoderm and an in situ change in amnion cell fate upon Smad5 deficiency, and links these to an unexpected gain-of-Bmp-function model that is supported by the exogenous rBMP4 phenocopy experiment. Amnion cultures may be exploited in the future to dissect and to clarify the Bmp signalling pathway that determines change in cell fate of the amnion.

We are grateful to M. Missoul and L. Desmet and to the 'mouse group' for assistance with mouse and ES cell work; to J. Korving for technical assistance; and to L. Umans and L. Cox for their stimulating work on other ongoing Smad5 projects in the mouse. We are indebted to M. M. Matzuk and H. Chang for the generation and collaborative analysis of the *Smad5*$^{m1/m1}$ mice in the past. We thank S. Chuva de Sousa-Lopes and C. Mummery for helpful discussions; F. Lemaigre and C. Pierreux for advice on embryo culture; and E. Delot, M. Jones and A. Surani for probes. E.A.B. thanks K. Steel for support. This work was supported by VIB, the University of Leuven (BOF/OT/00/41), the 'Interuniversity Attraction Poles Programme – Belgian Science Policy' project 5/35, project-based funding by the Fund of Scientific Research-Flanders (FWO-V; project G.0243.01) and the European Union (EU-grant T-Angiovasc QLG1-CT-2001-01032). E.A.B. thanks the IWT for a pre-doctoral fellowship. A.Z. was holder of a post-doc mandate of FWO-V.

Supplementary material

Supplementary material for this article is available at
http://dev.biologists.org/cgi/content/full/133/17/3399/DC1

References

Chang, H. and Matzuk, M. M. (2001). Smad5 is required for mouse primordial germ cell development. *Mech. Dev.* **104**, 61-67.

Chang, H., Huylebroeck, D., Verschueren, K., Guo, Q., Matzuk, M. M. and Zwijsen, A. (1999). Smad5 knockout mice die at mid-gestation due to multiple embryonic and extraembryonic defects. *Development* **126**, 1631-1642.

Chang, H., Zwijsen, A., Vogel, H., Huylebroeck, D. and Matzuk, M. M. (2000). Smad5 is essential for left-right asymmetry in mice. *Dev. Biol.* **219**, 71-78.

Delot, E., Bahamonde, M. E., Zhao, M. and Lyons, K. M. (2003). BMP signalling is required for septation of the outflow tract of the mammalian heart. *Development* **130**, 209-220.

de Sousa Lopes, S. M., Roelen, B. A., Monteiro, R. M., Emmens, R., Lin, H. Y., Li, E., Lawson, K. A. and Mummery, C. L. (2004). BMP signalling mediated by ALK2 in the visceral endoderm is necessary for the generation of primordial germ cells in the mouse embryo. *Genes Dev.* **18**, 1838-1849.

Dewulf, N., Verschueren, K., Lonnoy, O., Moren, A., Grimsby, S., Vande Spiegle, K., Miyazono, K., Huylebroeck, D. and ten Dijke, P. (1995). Expression of type I and type IB receptors for activin in midgestation mouse embryos suggests distinct functions in organogenesis. *Mech. Dev.* **52**, 109-123.

Donovan, P. J., Stott, D., Cairns, L. A., Heasman, J. and Wylie, C. C. (1986). Migratory and postmigratory mouse primordial germ cells behave differently in culture. *Cell* **44**, 831-838.

Dosch, R., Gawantka, V., Delius, H., Blumenstock, C. and Niehrs, C. (1997). Bmp-4 acts as a morphogen in dorsoventral mesoderm patterning in Xenopus. *Development* **124**, 2325-2334.

Downs, K. M. and Davies, T. (1993). Staging of gastrulating mouse embryos by morphological landmarks in the dissecting microscope. *Development* **118**, 1255-1266.

Downs, K. M. and Bertler, C. (2000). Growth in the pre-fusion murine allantois. *Anat. Embryol.* **202**, 323-331.

Downs, K. M., Gifford, S., Blahnik, M. and Gardner, R. L. (1998). Vascularization in the murine allantois occurs by vasculogenesis without accompanying erythropoiesis. *Development* **125**, 4507-4520.

Fox, N., Damjanov, I., Martinez-Hernandez, A., Knowles, B. B. and Solter, D. (1981). Immunohistochemical localization of the early embryonic antigen (SSEA-1) in postimplantation mouse embryos and fetal and adult tissues. *Dev. Biol.* **83**, 391-398.

Friedrich, G. and Soriano, P. (1991). Promoter traps in embryonic stem cells: a genetic screen to identify and mutate developmental genes in mice. *Genes Dev.* **5**, 1513-1523.

Fujiwara, T., Dunn, N. R. and Hogan, B. L. (2001). Bone morphogenetic protein 4 in the extraembryonic mesoderm is required for allantois development and the localization and survival of primordial germ cells in the mouse. *Proc. Natl. Acad. Sci. USA* **98**, 13739-13744.

Ginsburg, M., Snow, M. H. and McClaren, A. (1990). Primordial germ cells in the mouse embryo during gastrulation. *Development* **110**, 521-528.

Goumans, M. J., Zwijsen, A., van Rooijen, M. A., Huylebroeck, D., Roelen, B. A. and Mummery, C. L. (1999). Transforming growth factor-beta signalling in extraembryonic mesoderm is required for yolk sac vasculogenesis in mice. *Development* **126**, 3473-3483.

Gu, Z., Reynolds, E. M., Song, J., Lei, H., Feijen, A., Yu, L., He, W., MacLaughlin, D. T., van den Eijnden-van Raaij, J., Donahoe, P. K. et al. (1999). The type I serine/threonine kinase receptor ActRIA (ALK2) is required for gastrulation of the mouse embryo. *Development* **126**, 2551-2561.

Hayashi, K., Kobayashi, T., Umino, T., Goitsuka, R., Matsui, Y. and Kitamura, D. (2002). SMAD1 signalling is critical for initial commitment of germ cell lineage from mouse epiblast. *Mech. Dev.* **118**, 99-109.

Jones, C. M., Lyons, K. M. and Hogan, B. L. (1991). Involvement of Bone

Morphogenetic Protein-4 (BMP-4) and Vgr-1 in morphogenesis and neurogenesis in the mouse. *Development* **111**, 531-542.
Kinder, S. J., Tsang, T. E., Quinlan, G. A., Hadjantonakis, A. K., Nagy, A. and Tam, P. P. (1999). The orderly allocation of mesodermal cells to the extraembryonic structures and the anteroposterior axis during gastrulation of the mouse embryo. *Development* **126**, 4691-4701.
Kruzynska-Frejtag, A., Machnicki, M., Rogers, R., Markwald, R. R. and Conway, S. J. (2001). Periostin (an osteoblast-specific factor) is expressed within the embryonic mouse heart during valve formation. *Mech. Dev.* **103**, 183-188.
Lawson, K. A. and Hage, W. J. (1994). Clonal analysis of the origin of primordial germ cells in the mouse. *Ciba Found. Symp.* **182**, 68-84.
Lawson, K. A., Meneses, J. J. and Pedersen, R. A. (1991). Clonal analysis of epiblast fate during germ layer formation in the mouse embryo. *Development* **113**, 891-911.
Lawson, K. A., Dunn, N. R., Roelen, B. A., Zeinstra, L. M., Davis, A. M., Wright, C. V., Korving, J. P. and Hogan, B. L. (1999). Bmp4 is required for the generation of primordial germ cells in the mouse embryo. *Genes Dev.* **13**, 424-436.
Lechleider, R. J., Ryan, J. L., Garrett, L., Eng, C., Deng, C., Wynshaw-Boris, A. and Roberts, A. B. (2001). Targeted mutagenesis of Smad1 reveals an essential role in chorioallantoic fusion. *Dev. Biol.* **240**, 157-167.
Lyons, K. M., Pelton, R. W. and Hogan, B. L. (1989). Patterns of expression of murine Vgr-1 and BMP-2a RNA suggest that transforming growth factor-beta-like genes coordinately regulate aspects of embryonic development. *Genes Dev.* **3**, 1657-1668.
MacKenzie, A., Ferguson, M. W. and Sharpe, P. T. (1992). Expression patterns of the homeobox gene, Hox-8, in the mouse embryo suggest a role in specifying tooth initiation and shape. *Development* **115**, 403-420.
Miki, T., Lehmann, T., Cai, H., Stolz, D. B. and Strom, S. C. (2005). Stem cell characteristics of amniotic epithelial cells. stem cells. *Stem Cells* **23**, 1549-1559.
Mishina, Y., Crombie, R., Bradley, A. and Behringer, R. R. (1999). Multiple roles for activin-like kinase-2 signalling during mouse embryogenesis. *Dev. Biol.* **213**, 314-326.
Monaghan, A. P., Davidson, D. R., Sime, C., Graham, E., Baldock, R., Bhattacharyo, S. S. and Hill, R. E. (1991). The Msh-homeobox genes define domains in the developing vertebrate eye. *Development* **112**, 1053-1061.
Nakamura, K., Shirai, T., Morishita, S., Uchida, S., Saeki-Miura, K. and Makishima, F. (1999). p38 mitogen-activated protein kinase functionally contributes to chondrogenesis induced by growth/differentiation factor-5 in ATDC5 cells. *Exp. Cell Res.* **250**, 351-363.
Ohinata, Y., Payer, B., O'Carroll, D., Ancelin, K., Ono, Y., Sano, M., Barton, S. C., Obukhanych, T., Nussenzweig, M., Tarakhovsky, A. et al. (2005). Blimp1 is a critical determinant of the germ cell lineage in mice. *Nature* **436**, 207-213.
Okamura, D., Hayashi, K. and Matsui, Y. (2005). Mouse epiblasts change responsiveness to BMP4 signal required for PGC formation through functions of extraembryonic ectoderm. *Mol. Reprod. Dev.* **70**, 20-29.
Parameswaran, M. and Tam, P. P. (1995). Regionalisation of cell fate and morphogenetic movement of the mesoderm during mouse gastrulation. *Dev. Genet.* **17**, 16-28.
Qi, X., Li, T. G., Hao, J., Hu, J., Wang, J., Simmons, H., Miura, S., Mishina, Y. and Zhao, G. Q. (2004). BMP4 supports self-renewal of embryonic stem cells by inhibiting mitogen-activated protein kinase pathways. *Proc. Natl. Acad. Sci. USA* **101**, 6027-6032.
Saitou, M., Barton, S. C. and Surani, M. A. (2002). A molecular programme for the specification of germ cell fate in mice. *Nature* **418**, 293-300.
Sakuragawa, N., Kakinuma, K., Kikuchi, A., Okano, H., Uchida, S., Kamo, I., Kobayashi, M. and Yokoyama, Y. (2004). Human amnion mesenchyme cells express phenotypes of neuroglial progenitor cells. *J. Neurosci. Res.* **78**, 208-214.
Schöler, H. R. (1991). Octamania: the POU factors in murine development. *Trends Genet.* **7**, 323-329.
Schoonjans, L., Kreemers, V., Danloy, S., Moreadith, R. W., Laroche, Y. and Collen, D. (2003). Improved generation of germline-competent embryonic stem cell lines from inbred mouse strains. *Stem Cells* **21**, 90-97.
Shi, Y. and Massagué, J. (2003). Mechanisms of TGF-beta signalling from cell membrane to the nucleus. *Cell* **113**, 685-700.
Solloway, M. J. and Robertson, E. J. (1999). Early embryonic lethality in Bmp5;Bmp7 double mutant mice suggests functional redundancy within the 60A subgroup. *Development* **126**, 1753-1768.
Tamagawa, T., Ishiwata, I. and Saito, S. (2004). Establishment and characterization of a pluripotent stem cell line derived from human amniotic membranes and initiation of germ layers in vitro. *Hum. Cell* **17**, 125-130.
Tanaka, S. S., Nagamatsu, G., Tokitake, Y., Kasa, M., Tam, P. P. and Matsui, Y. (2004). Regulation of expression of mouse interferon-induced transmembrane protein like gene-3, Ifitm3 (mil-1, fragilis), in germ cells. *Dev. Dyn.* **230**, 651-659.
Tanaka, S. S., Yamaguchi, Y. L., Tsoi, B., Lickert, H. and Tam, P. P. (2005). IFITM/Mil/fragilis family proteins IFITM1 and IFITM3 play distinct roles in mouse primordial germ cell homing and repulsion. *Dev. Cell* **9**, 745-756.
Tremblay, K. D., Dunn, N. R. and Robertson, E. J. (2001). Mouse embryos lacking Smad1 signals display defects in extra-embryonic tissues and germ cell formation. *Development* **128**, 3609-3621.
Umans, L., Vermeire, L., Francis, A., Chang, H., Huylebroeck, D. and Zwijsen, A. (2003). Generation of a floxed allele of Smad5 for cre-mediated conditional knockout in the mouse. *Genesis* **37**, 5-11.
Van Eynde, A., Nuytten, M., Dewerchin, M., Schoonjans, L., Keppens, S., Beullens, M., Moons, L., Carmeliet, P., Stalmans, W. and Bollen, M. (2004). The nuclear scaffold protein NIPP1 is essential for early embryonic development and cell proliferation. *Mol. Cell. Biol.* **24**, 5863-5874.
Vincent, S. D., Dunn, N. R., Sciammas, R., Shapiro-Shalef, M., Davis, M. M., Calame, K., Bikoff, E. K. and Robertson, E. J. (2005). The zinc finger transcriptional repressor Blimp1/Prdm1 is dispensable for early axis formation but is required for specification of primordial germ cells in the mouse. *Development* **132**, 1315-1325.
Winnier, G., Blessing, M., Labosky, P. A. and Hogan, B. L. (1995). Bone morphogenetic protein-4 is required for mesoderm formation and patterning in the mouse. *Genes Dev.* **9**, 2105-2116.
Yang, X., Castilla, L. H., Xu, X., Li, C., Gotay, J., Weinstein, M., Liu, P. P. and Deng, C. X. (1999). Angiogenesis defects and mesenchymal apoptosis in mice lacking SMAD5. *Development* **126**, 1571-1580.
Ying, Q. L., Nichols, J., Chambers, I. and Smith, A. (2003). BMP induction of Id proteins suppresses differentiation and sustains embryonic stem cell self-renewal in collaboration with STAT3. *Cell* **115**, 281-292.
Ying, Y. and Zhao, G. Q. (2001). Cooperation of endoderm-derived BMP2 and extraembryonic ectoderm-derived BMP4 in primordial germ cell generation in the mouse. *Dev. Biol.* **232**, 484-492.
Ying, Y., Liu, X. M., Marble, A., Lawson, K. A. and Zhao, G. Q. (2000). Requirement of Bmp8b for the generation of primordial germ cells in the mouse. *Mol. Endocrinol.* **14**, 1053-1063.
Ying, Y., Qi, X. and Zhao, G. Q. (2001). Induction of primordial germ cells from murine epiblasts by synergistic action of BMP4 and BMP8B signalling pathways. *Proc. Natl. Acad. Sci. USA* **98**, 7858-7862.
Zhang, H. and Bradley, A. (1996). Mice deficient for BMP2 are nonviable and have defects in amnion/chorion and cardiac development. *Development* **122**, 2977-2986.
Zhao, G. Q. (2003). Consequences of knocking out BMP signalling in the mouse. *Genesis* **35**, 43-56.
Zhao, P., Ise, H., Hongo, M., Ota, M., Konishi, I. and Nikaido, T. (2005). Human amniotic mesenchymal cells have some characteristics of cardiomyocytes. *Transplantation* **79**, 528-535.

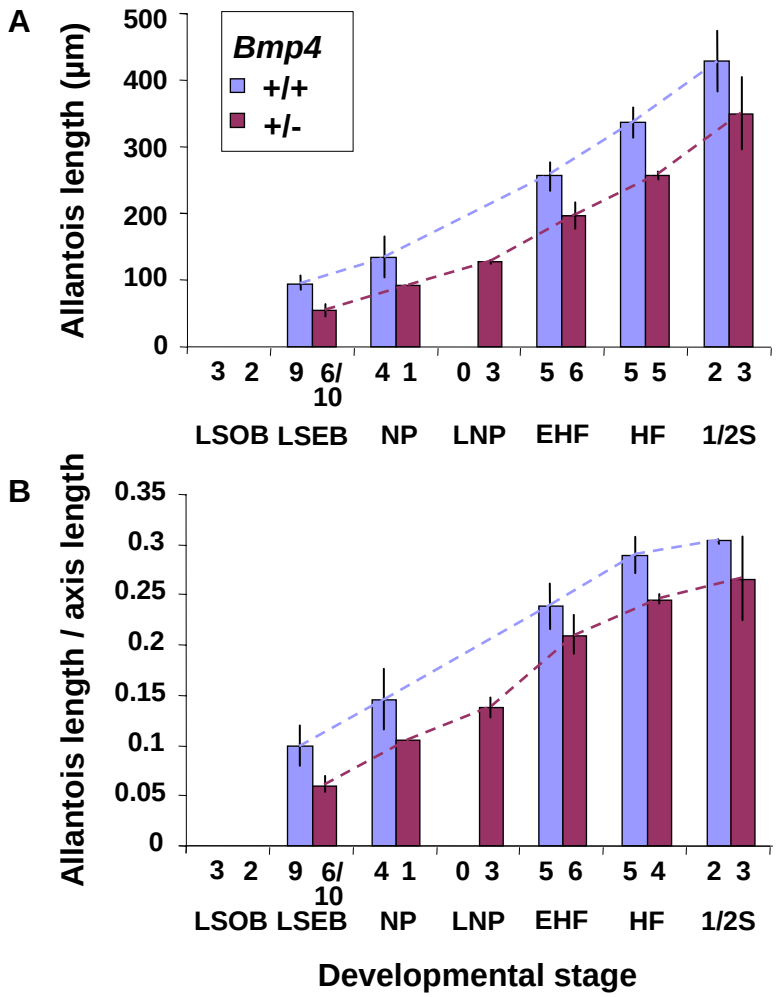
A
Allantois length (µm)
500
400
300
200
100
0
Bmp4
+/+
+/-
3 2
9 6/10
4 1
0 3
5 6
5 5
2 3
LSOB LSEB
NP
LNP
EHF
HF
1/2S
B
Allantois length / axis length
0.35
0.3
0.25
0.2
0.15
0.1
0.05
0
3 2
9 6/10
4 1
0 3
5 6
5 4
2 3
LSOB LSEB
NP
LNP
EHF
HF
1/2S
Developmental stage

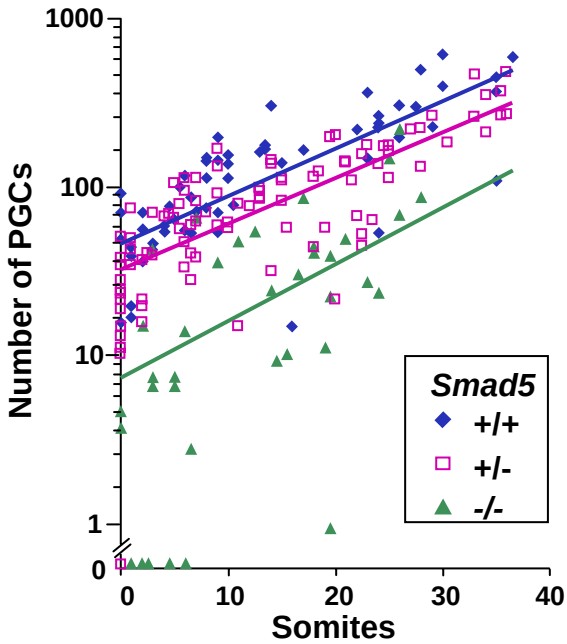
1000
100
10
1
0
Number of PGCs
0
10
20
30
40
Somites
Smad5
+/+
+/-
-/-